

PAPER • OPEN ACCESS

Research on Strain Distribution Detection Method of Freeform Surface Based on FBG Array

To cite this article: Zhichao Liu *et al* 2019 *IOP Conf. Ser.: Mater. Sci. Eng.* **490** 062040

View the [article online](#) for updates and enhancements.

Research on Strain Distribution Detection Method of Freeform Surface Based on FBG Array

Zhichao Liu^{*}, Maosheng Hou, Xuezhu Lin, Tao Liu, Lili Guo, Lijuan Li

School of Optoelectronic Engineering, Changchun University of Science and Technology, Changchun, Jilin, China

^{*}Corresponding author e-mail: s20070384@163.com

Abstract. In order to obtain the strain distribution of the free-form surface to be tested and reduce the difficulty of assembling large-scale curved structures, a free-form surface strain distribution detection method based on FBG array was designed. The system consists of a laser, a coupler, a demodulator, and an FBG array. The strain distribution and displacement offset of the test specimen under five different force conditions are simulated and analyzed. The simulation results show that the strain distribution is related to the position, size and surface structure of the applied force. The experiment was tested on a 3 mm aluminum plate and compared to the simulation data. 1. The experimental results show that the maximum strain is $24.7\mu\epsilon$ and the minimum strain is $2.8\mu\epsilon$. The difference in strain at the same curvature position is significant. It verifies the feasibility of solving the displacement field distribution by the strain field distribution.

1. Introduction

In recent years, optical fiber sensing networks have been widely used in various industries. FBG (Fiber Bragg grating) ^[1-3] is a sensor that can form an FBG array detection structure for measurement of bending, displacement, strain, temperature, and so on. It is widely used in aircraft, motor trains, high-end cars and other targets ^[4-6]. For the detection of free-form surfaces, in order to effectively analyze the strain distribution and solve the displacement deviation by the strain distribution, the effective assembly of the free-form surface structure can be realized.

The strain measurement methods for free-form surfaces are direct measurement ^[7,8] and visual measurement ^[9,10]. Direct measurement is to directly measure the data by attaching strain gauges or FBG to the object to be tested ^[11]. The advantage of this method is that the direct measurement accuracy is high, and the position and quantity of the measurement points can be arranged according to requirements. Strain gauges are not suitable when there is increased electromagnetic interference in the test environment. Visual measurement is mainly divided into laser scanning and photographing. Laser scanning enables non-contact measurement with high measurement accuracy, but has certain requirements for test space ^[12]. The photographing method is fast, mainly realized by digital image processing, but the test environment is high and the test position is unobstructed. In contrast, in the detection process of large-sized free-form surface structures, FBG arrays can lay out test points in a wide range. It is immune to electromagnetic interference and has few special requirements for the test environment due to its small size.



This paper studies the free-form surface strain distribution detection system based on FBG array, quantitative calculation of the reference position and deformation degree of the free-form surface, in order to provide better data support for digital assembly.

2. System structure

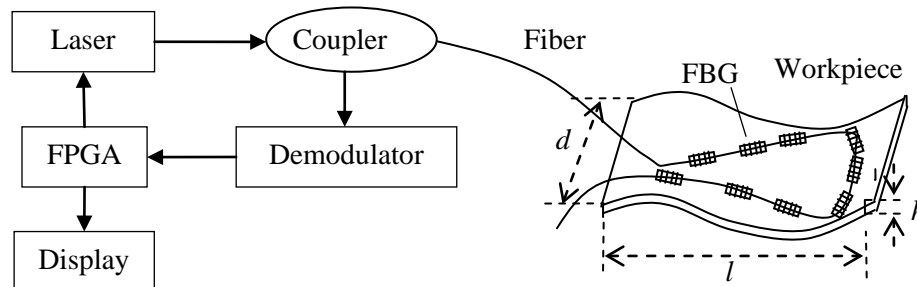


Fig.1 FBG array test system

The system structure is shown in Figure 1. The laser enters the coupler through the fiber and is then transmitted to the FBG array. The FBG array on the free-form surface acquires the wavelength offset data at the corresponding position, respectively. The FBG sensing array is placed from top to bottom and then placed on the device to be tested from bottom to top. The echo enters the demodulator through the coupler to complete the solution, and the distribution data of the strain field is obtained for correcting the assembly parameters.

Let the temperature of the test environment not change, the echo wavelength is λ_B , the echo wavelength offset value is $\Delta\lambda_B$, the elastic light coefficient is P_e , the test specimen thickness is h , the test position size is L , and the deformation amount is ΔL . The wavelength offset data for each FBG detector is only related to its dependent variable and has:

$$\frac{\Delta\lambda_B}{\lambda_B} = (1 - P_e) \frac{\Delta L}{L} \quad (1)$$

It can be seen from the above equation that when the initial center wavelength is known and the test echo value is measurable, the amount of deformation at that position can be calculated. Correction of the position information of the digital assembly can be achieved by calculating the amount of deformation. The set of measured points can be expressed as

$$U'(x, y, z) = [1 - f(\varepsilon)] \cdot U(x, y, z) \quad (2)$$

Where $U(x, y, z)$ is a set of digital modulus points, and $\Delta U(x, y, z)$ is a deviation correction value. When the strain model is obtained through testing, the set of measured points can be calculated to realize the auxiliary assembly.

3. Simulation analysis

Solidworks software is used to simulate the strain field of the complex curved test specimen and the displacement field after deformation of the test specimen for the analysis of the strain field of the test specimen. The system mainly analyzes the strain distribution caused by the dead weight and the station fixture. It is distributed and analyzed at different positions of the test specimen. The simulation results are shown in Figure 2.

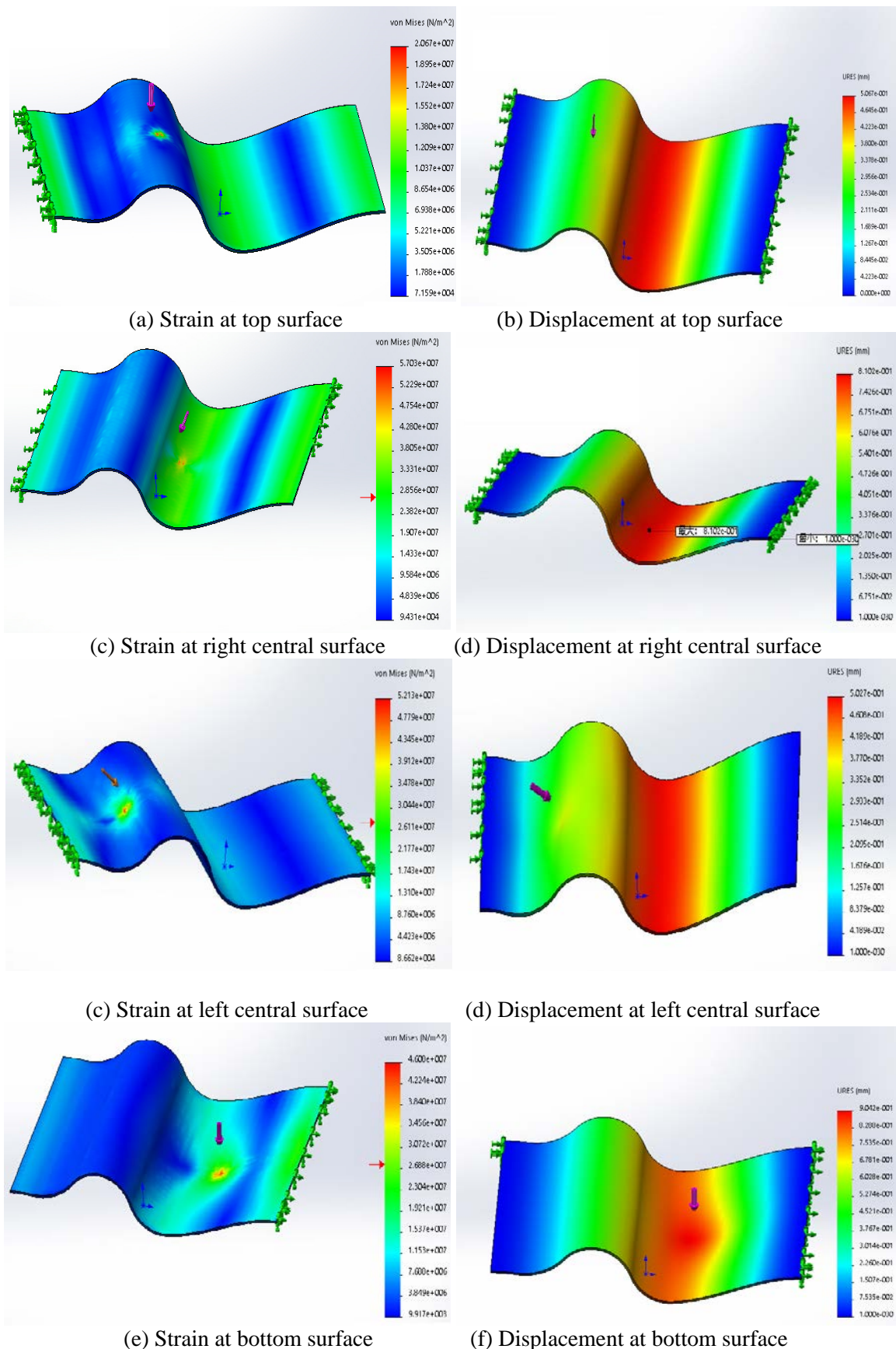


Fig.2 Simulation of strain and displacement in different situations

The material for simulating the test piece is aluminum, the size is 20mm×10mm×3mm ($l \times d \times h$), and the external force is $F=50\text{N}$. It can be seen from Fig. 2 (a) and (b) that the maximum micro-displacement deformation is 0.5067 mm when the top is subjected to force, and the deformation zone is mainly concentrated on the lower curved section. It can be seen from Fig. 2 (c) and (d) that the maximum micro-displacement deformation is 0.8102 mm when the right middle portion is stressed, and the deformation region is mainly concentrated on the lower curved surface segment. It can be seen from Fig. 2(e) and (f) that the maximum micro-displacement deformation is 0.3725 mm when the left middle part is stressed, and the deformation zone is mainly concentrated in the attachment point of the force application point. It can be seen from Fig. 2(g) and (h) that the maximum micro-displacement deformation amount is 0.9042 mm when the bottom is subjected to force, and the deformation zone is mainly concentrated on the side of the force application point near the arch surface. It is worth noting that the first three sets of test data will cause the displacement deviation of the entire segment of the lower surface segment, while the displacement deviation generated by the last set of data is mainly concentrated on the applied point. It can be seen that the distribution of micro-displacements caused by different stress application points is not completely determined by the point of application. In the FBG array distribution design, it is necessary to consider the shape of the device to be tested. According to the simulation analysis results, the FBG array has three sets of distributions from the arch surface to the bottom surface for better obtaining strain data.

4. Experiment

DFB broadband light source, fiber grating demodulator and FBG sensing array were used in the experimental system. The FBG probe array is arranged on the object to be tested according to the distribution pattern of FIG. 1, and the object to be tested is an aluminum plate of 20mm×10mm×3mm. With a force of 50 N applied to the top, the FBG array is distributed as shown in Fig. 1. The test data of the same position is collected five times each time, and the bottom force is taken as an example. The strain test values of the FBG array are shown in Table 1.

Table 1. test data of the strain

No.	Coordinate position(x,y) /mm	Simulation value / $\mu\epsilon$	measured value / $\mu\epsilon$	Error / $\mu\epsilon$
1	(6.7, 3.2)	26.4	24.7	1.7
2	(11.4, 6.5)	20.3	18.6	1.7
3	(15.6, 8.7)	10.1	8.7	1.4
4	(17.3, 8.7)	4.3	6.1	1.8
5	(17.3, 6.5)	3.6	4.3	0.7
6	(17.3, 3.2)	2.7	3.7	1.0
7	(15.6, 2.5)	3.9	2.8	1.1
8	(11.4, 2.5)	12.6	11.4	1.2
9	(6.7, 2.5)	21.2	19.8	1.4

As shown in Table 1, there are large differences in the micro-variables of the applied force points at different positions of the workpiece. In the first group of FBGs, measured value of the No. 1 FBG is the largest (26.4 $\mu\epsilon$), the No. 2 FBG is similar to the No. 9 FBG change; in the second group FBG, the overall test data is similar. It can be seen from the system test data that the closer the test point shape variable is to the point of stress application. The dependent variable also receives the effect of the structural shape. The overall average error of the test data is 1.52. According to different coordinate positions, the system test shows the distribution trend of strain. Only one set of test data is given in Table 1. The other test data is more and not all written. All strain distributions are redrawn by means of data reconstruction to obtain a positional offset curve calculated from the strain field distribution, as shown in Figure 3.

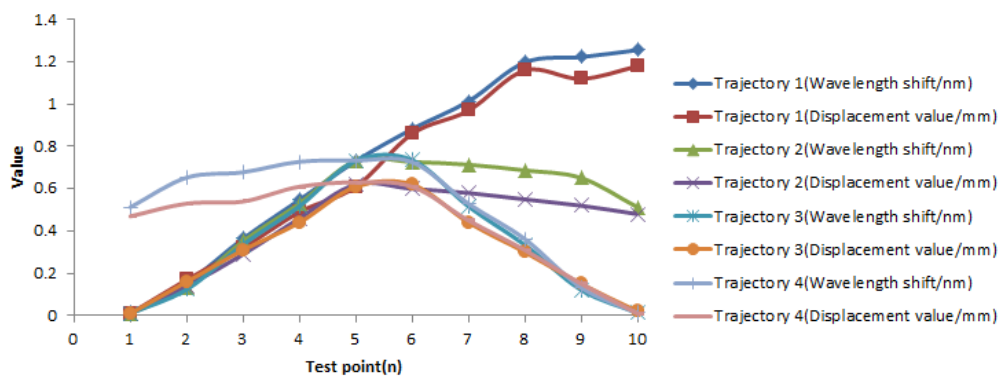


Fig.3 Error from FBG array

According to the experimental reconstruction data, there is a significant correlation between strain and displacement offset. At different test locations, the stress changes at the same point will have significantly different differences, and it can be seen that such a strain distribution can affect the displacement offset. This is also the main basis for solving the displacement field distribution by the strain field distribution. Finally, experimental and simulation calculations can effectively reflect the feasibility of the system.

5. Conclusion

The strain field and displacement offset of free-form surface test specimen are tested by FBG sensing array. The strain distribution and displacement offset of the workpiece under different force conditions are calculated by simulation. The main parameters affecting the displacement offset are verified by experiments and the error distribution curve is given. The system has a stable test effect on the strain field and the displacement offset of the free-form surface workpiece.

Acknowledgments

This work was financially supported by the National Science Foundation of China (Theoretical Model and Experimental Research on the Novel FBG Sensing System based on the Fusion Algorithm”, No. 61703056).

References

- [1] DUNCAN R G, FROGCATT M E, KREGER S T, et al. High-accuracy fiber-optic shape sensing [C]. International Symposium on Smart Structure & Materials & Nondestructive Evaluation & Health Monitoring, 2007: 65301s-11.
- [2] CLEMENTS G M. Fiber optic sensor for precision 3-D position measurement: US, US6888623[P]. 2005.
- [3] Almazyad, A.S.; Seddiq, Y.M.; Alotaibi, A.M.; Al-Nasheri, A.Y.; BenSaleh, M.S.; Obeid, A.M.; Qasim, S.M. A proposed scalable design and simulation of wireless sensor network-based long-distance water pipeline leakage monitoring system. *Sensors* 2014, 14, 3557–3577.
- [4] Xinhua Yao, Congcong Luan, Deming Zhang, Liujian Lan, Jianzhong Fu. Evaluation of carbon fiber-embedded 3D printed structures for strengthening and structural-health monitoring[J]. *Materials & Design*, 2017, 114.
- [5] Spirin, V.V. Fiber Bragg Grating sensor for petroleum hydrocarbon leak detection. *Optics and Laser in Engineering*, 2000, 5, 497–503.
- [6] Yasser M. Al-Anany, Michael J. Tait. Fiber reinforced elastomeric isolators for the seismic isolation of bridges[J]. *Composite Structures*, 2017, 160.
- [7] Khan, M.M.; Panwar, N.; Dhawan, R. Modified cantilever beam shaped FBG based accelerometer with self temperature compensation. *Sensors & Actuators A Physical*, 2014, 205, 79–85.
- [8] Liu, Z.; Yang, J.; Wang, G. Research on Spectrum Correction Algorithm of Temperature Measurement System Based on FBG. *Spectroscopy and Spectral Analysis*, 2014, 7, 1793-1796.

- [9] Sumayyah, M.I.; Mohammed, R.H.A.; Aiman, I. Sensitivity and stability characterization of linear cavity erbium-doped fiber laser for pressure measurement. *Microwave Opt. Technol. Lett.*, 2012, 11, 2447–2449.
- [10] Liu, Z.; Yang, J.; Zhang, L.; Wang, G. Granary Temperature Measurement Network Based on Chirped FBG. *Spectroscopy and Spectral Analysis*, 2016, 10, 3377–3380.
- [11] Daniel, L.; Veronica, M.S.; Manuel, L.A. High-resolution sensor system using a random distributed feedback fiber laser. *J. Lightwave Technol.*, 2016, 19, 4596–4602.
- [12] Xu J.; Yang, D.; Qin C.; Jiang, Y.; Sheng, L.; Jia X.; Bai Y.; Shen X.; Wang, H.; Deng X.; Xu L.; Jiang S. Study and Test of a New Bundle-Structure Riser Stress Monitoring Sensor Based on FBG. *Sensors*, 2015, 15, 29648–29660.